

PACS numbers: 42.55.Ks; 33.20.Vq
DOI: 10.1070/QE2003v033n09ABEH002504

Detection of vibrationally excited O_2 in the active medium of a chemical oxygen – iodine laser

V.N. Azyazov, I.O. Antonov, S.Yu. Pichugin, V.S. Safonov, M.I. Svistun, N.I. Ufimtsev

***Abstract*. The presence of vibrationally excited oxygen in the active medium of a chemical oxygen – iodine laser is discovered using the emission technique. Using the analysis of the luminescence spectra of oxygen molecules on $O_2(b^1\Sigma_g^+, v = i) \rightarrow O_2(X^3\Sigma_g^-, v' = i)$ ($i = 0, 1, 2$) electronic vibrational – rotational transitions, it is shown that $\sim 22\,\%$ of $O_2(b^1\Sigma_g^+)$ molecules are at the first vibrational level and $\sim 10\,\%$ are at the second one. Moreover, due to the fast EE energy exchange, a mean number of vibrational quanta per one molecule in each of the $O_2(X^3\Sigma_g^-)$, $O_2(a^1\Delta_g)$ and $O_2(b^1\Sigma_g^+)$ components is approximately the same and amounts to 30 %– 40 %.**

Keywords: *oxygen, vibrational excitation, emission spectrum, oxygen – iodine laser*.

1. Introduction

The electron-energy deactivation in the active medium of a chemical oxygen – iodine laser (COIL) leads to the formation of vibrationally excited O_2, H_2O, and I_2 molecules in the following processes:

$$O_2(a) + O_2(a) \rightarrow O_2(b, v) + O_2(X, v'), \quad (1)$$

$$O_2(a) + I^* \rightarrow O_2(b, v) + I, \quad (2)$$

$$O_2(b) + H_2O \rightarrow O_2(a, v) + H_2O(v'), \quad (3)$$

$$I^* + H_2O \rightarrow I + H_2O(v), \quad (4)$$

$$I^* + I_2(X) \rightarrow I + I_2(X, v). \quad (5)$$

Hereafter, $O_2(X)$, $O_2(a)$, and $O_2(b)$ are the oxygen molecules in the $X^3\Sigma_g^-$, $a^1\Delta_g$, and $b^1\Sigma_g^+$ states; I, and I^* are iodine atoms in the $^2P_{3/2}$ and $^2P_{1/2}$ states; $I_2(X)$, $I_2(A')$, $I_2(A)$, and $I_2(B)$ are iodine molecules in the $X^1\Sigma_g^+$, $A'^3\Pi_{2u}$, $A^3\Pi_{1u}$, and $B^3\Pi_{0_u^+}$ states. Vibrationally excited oxygen $O_2(b, v)$ is produced in pooling reaction (1) with yield probabilities $\gamma_0 = 0.32$ for $v = 0$, $\gamma_1 = 0.04$ for $v = 1$, and $\gamma_2 = 0.64$ for $v = 2$ [1]. The energy-defect distribution between the products of pooling reaction (2) is unknown. The formation probability of the $H_2O(001)$ vibrationally excited molecule in reaction (3) is 0.1 [2]. Calculations show that the greater part of the energy released in reactions (1) – (3) is transferred to the vibrational degrees of freedom of the reactants [3]. Vibrationally excited $H_2O(002)$ molecules are produced in reaction (4) [4]. The formation of vibrationally excited iodine $I_2(X, 25 \leqslant v \leqslant 43)$ in reaction (5) was discovered in Refs [5, 6].

Vibrationally excited oxygen can play an important role in the formation of the COIL active medium, especially during the I_2 dissociation. It was assumed in Refs [7, 8] that excited iodine electronic states $I_2(A)$ and $I_2(A')$ are intermediate in the iodine dissociation process. They are populated in collisions with vibrationally excited singlet oxygen in the processes

$$O_2(a, v = 1) + I_2(X) \rightarrow O_2(X) + I_2(A'), \quad (6)$$

$$O_2(a, v = 2) + I_2(X) \leftrightarrow O_2(X) + I_2(A). \quad (7)$$

The EE energy exchange between O_2 and I_2 was observed in several works. $I_2(A)$ and $I_2(A')$ molecules were detected in the presence of singlet oxygen [9, 10]. The EE energy transfer from $I_2(A)$ and $I_2(A')$ molecules to O_2 was observed in Ref. [11]. The rates of $I_2(A')$ deactivation on O_2, H_2O, and N_2 molecules were measured in Ref. [12]. It was determined in Ref. [12] that the rate of $I_2(A')$ deactivation on O_2 is higher than on H_2O. This was explained by the EE energy transfer from iodine to oxygen. As is well known, the I_2 dissociation process in the $O_2(a)$ medium is accompanied by an intense luminescence of molecular iodine on the $I_2(B) \rightarrow I_2(X)$ transition in the visible spectral region with a maximum at 580 nm. The analysis of the luminescence spectra shows that the $I_2(B, 20 \leqslant v \leqslant 25)$ vibrationally excited states are populated [13]. They can be populated in the following sequence of reactions. At the first stage, the $I_2(A)$ and $I_2(A')$ electronic states are excited in processes (6) and (7). At the second stage, the $I_2(B, 20 \leqslant v \leqslant 25)$ levels are populated in collisions with $O_2(a)$.

Detecting the vibrationally excited oxygen is a complex problem because O_2 molecules have no intrinsic dipole moment [14]. The electronic and vibrational states of particles are excited in the COIL active medium. Their emission spectra contain much information on the rates of

V.N. Azyazov, I.O. Antonov, S.Yu. Pichugin, V.S. Safonov, M.I. Svistun, N.I. Ufimtsev P.N. Lebedev Physics Institute, Samara Branch, Russian Academy of Sciences, ul. Novo-Sadovaya 221, 443011 Samara, Russia; e-mail: azyazov@fian.smr.ru; web-site: http//www.fian.smr.ru

Received 17 February 2003
Kvantovaya Elektronika **33** (9) 811 – 816 (2003)
Translated by A.S. Seferov

the occurring processes and quantitative data on the concentration of excited particles. The fraction of vibrationally excited oxygen at the exit of the chemical generator of singlet oxygen was measured by the emission technique [15]. The comparison of the intensities of oxygen-dimole emission bands at $\lambda = 579$ and 634 nm has shown that the fraction of oxygen at the first vibrational level is essentially nonequilibrium and amounts to 2 %. The technique used in Ref. [15] is inapplicable to the detect vibrationally excited O_2 in the COIL active medium because the iodine luminescence at the $I_2(B) \rightarrow I_2(X)$ transition overlaps the oxygen-dimole emission bands.

Calculations show that a mean number of vibrational quanta per one O_2 molecule in the COIL active medium may reach several tens of percent [16], but this fact has not been confirmed experimentally. The aim of this work is to detect and determine the amount of vibrationally excited oxygen in the COIL active medium from the luminescence spectra of oxygen at the transitions

$$O_2(b, v = 0) \rightarrow O_2(X, v' = 0) + hv_8, \quad (8)$$

$$O_2(b, v = 1) \rightarrow O_2(X, v' = 1) + hv_9, \quad (9)$$

$$O_2(b, v = 2) \rightarrow O_2(X, v' = 2) + hv_{10}. \quad (10)$$

2. Experimental

The luminescence bands of oxygen corresponding to transitions (8)–(10) were measured using an experimental setup shown in Fig. 1. Electronically excited $O_2(a)$ molecules were produced in a chemical jet generator of singlet oxygen. Its reaction chamber (*3*) was a cylindrical cavity 12 mm in diameter and 10 cm in height. The gas–liquid generator operated in the counterflow regime. Gaseous Cl_2 was injected into the bottom part of the reaction zone through two oppositely positioned holes. The basic hydrogen peroxide solution was injected into the upper part of the reaction zone. This solution was prepared in a tank (*2*) from 1.2 L of H_2O_2 and 0.8 L of a KOH solution with concentrations of 37 wt % and 14.5 mol L^{-1}, respectively. The temperature of the solution was maintained at a level of –15 °C. Before the start, the solution was degassed by evacuating the feeding tank (*2*). The tank was then filled with compressed air. Under the action of a pressure difference, a liquid flow was accelerated and ejected in the form of free jets, into the reaction zone (*3*). The pressure difference across the jet injector (*4*) was 1.5 atm. The injector (*4*) consisted of 43 stainless-steel tubes 25 mm long with a 0.5-mm inner diameter. The jet velocity in the reactor zone was 5 m s^{-1}. The gas velocity in the reaction zone was controlled by a throttling slit valve (*5*) installed at the generator exit.

The measuring cell made of organic glass (Fig. 1b) was joined directly to the generator unit. The gas channel (*10*) of the measuring cell was 5 cm wide and 1.5 cm high. Nine nozzles (*9*) for injecting the iodine flow were positioned 16 cm away from the throttling slit valve (*5*). The height, width, and length along the flow of each nozzle were 1.5, 0.25, and 1.0 cm, respectively. The copper walls of the nozzles were 0.15 mm thick. The nozzles' outer surfaces were coated with a thin layer of polymethyl methacrylate (PMMA) dissolved in chloroform. The distance between the

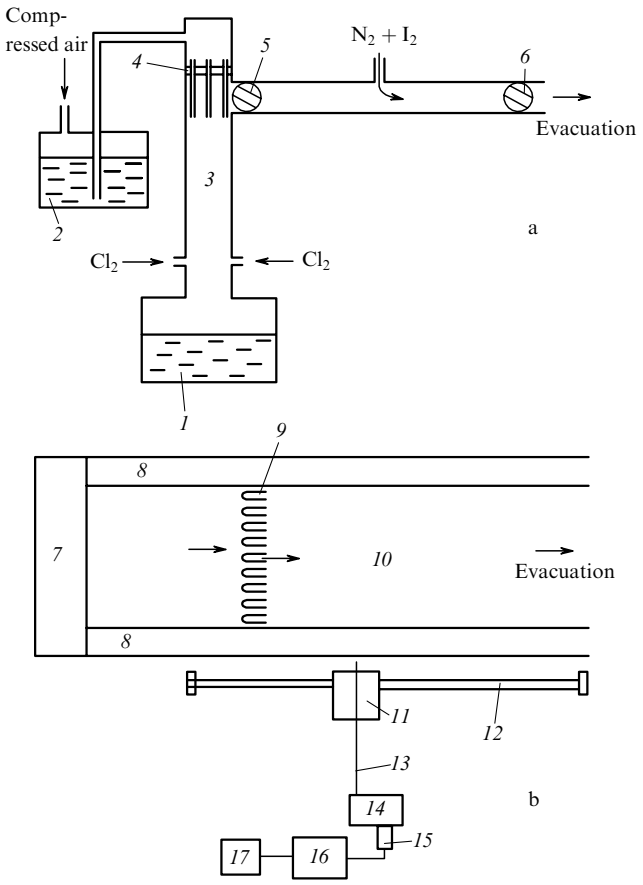

Figure 1. (a) General view and (b) top view of the experimental setup: (*1*) receiving tank; (*2*) feeding tank; (*3*) generator reaction zone; (*4*) jet injector; (*5*, *6*) throttling slit valve; (*7*) singlet-oxygen generator; (*8*) walls of the measurement cell; (*9*) nozzles for injecting the iodine flow; (*10*) gas channel of the measurement cell; (*11*) movable platform; (*12*) movable-platform guide; (*13*) optical fibre; (*14*) monochromator; (*15*) FEU-69b photomultiplier; (*16*) U7-1 amplifier, and (*17*) PC with a built-in ADC board.

lateral surfaces of adjacent nozzles was 2.5 mm. The distance from the edge of the nozzle assembly to the throttling slit valve (*6*) that controlled the gas velocity in the measurement cell was 24 cm.

Nitrogen was used as a carrier gas for iodine vapours. The iodine flow was injected into the nozzles through 1.5-mm-diameter nickel tubes mounted in them 7 mm upstream from the nozzle edge. Five 0.5-mm-diameter holes were drilled on each tube's side perpendicular to the oxygen flow. The gas-channel cross section that was not occupied by the nozzles was used to form plane–parallel oxygen jets. Thus, alternating iodine and oxygen jets with equal cross sections of 2.5×15 mm appeared behind the nozzle assembly. To avoid iodine condensation on the walls of the nozzle assembly, its temperature was maintained at 40 °C.

The gas-medium emission passed through the wall of cell (*8*), entered an optical fiber (*13*), and was transmitted through it to the entrance slit of a monochromator (*14*). The light flux at the monochromator exit was detected by a photomultiplier (*15*). Its output signal was amplified by a precision amplifier (*16*) with a passband of 0–10 Hz.

The gas pressure in the singlet-oxygen generator and the measuring cell was measured by Sapfir pressure gauges. The vapour generator of gaseous iodine and the system for its

flow-rate measurements were similar to those used in Ref. [17]. Data were collected and processed using a personal computer (PC) (*17*) with a built-in ADC board. The monochromator scanning system generated electric pulses that were also fed to the PC and served as references in the wavelength calibration of spectra. The spectrum scanning rate was 80 nm min^{-1}. The generator operating-cycle duration was ~ 40 s, being determined by the supply of the solution in the feeding tank (*2*).

In all our experiments, the flow rates of chlorine (G_{Cl_2}) and buffer gas N_2 that carried I_2 vapours were the same: $G_{Cl_2} = G_{N_2} = 2.5$ mmol s^{-1}. Therefore, the velocities of oxygen and iodine gas jets behind the nozzle assembly can be considered approximately equal. The mean calculated gas velocity in the measurement cell behind the nozzles was ~ 40 m s^{-1}. The fraction of $O_2(a)$ at the singlet-oxygen generator output was $\eta_a = N_a/N_{O_2} \approx 60 \pm 10$ %, and the degree of Cl_2 utilisation in the generator exceeded 95 % [N_a, and N_{O_2} are the concentrations of $O_2(a)$ and oxygen in all electronics states].

3. Results and discussion

The gas mixture under study had a composition close to the COIL active medium. Measurements showed that its emission spectrum in the range of 480–820 nm is a broad band of molecular iodine with a maximum at 580 nm. This band overlaps several luminescence bands of oxygen. The iodine luminescence intensity in the region of 750–800 nm was weaker than the intensity emitted by oxygen at the transitions (8) – (10). Fig. 2 shows the intensity signals I detected between 757 and 785 nm for two values of the initial fraction of molecular iodine $\eta_{I_2} = G_{I_2}/G_{Cl_2} = 0.83$ % and 0.31 % (G_{I_2} is the I_2 flow rate) at gas pressures in the singlet-oxygen generator $p_g \approx 35$ Torr and in the measurement cell $p_c \approx 3$ Torr at a distance $L = 5$ cm from the end of the nozzle assembly along the flow. Symbols $R(bi - Xi)$ and $P(bi - Xi)$ denote the profiles of the R and P rotational branches for three electronic–vibrational–rotational transitions (8)–(10) of O_2 molecules (i is vibrational-level number). The emission spectra were measured with a wavelength resolution of 0.5 nm.

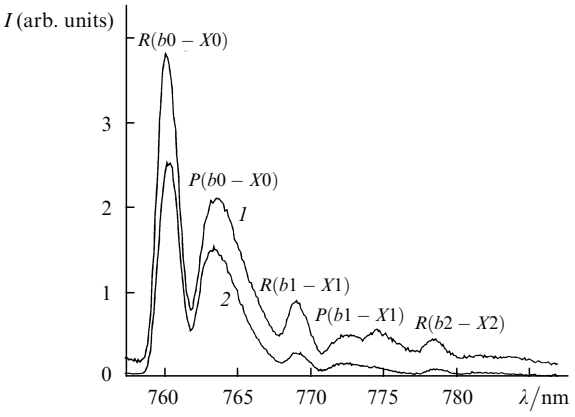

Figure 2. Emission spectrum I at $N_2 : O_2 : H_2O = 100 : 100 : 4$, $p_g \approx 35$ Torr, $p_c = 3$ Torr, and $L = 5$ cm for $\eta_{I_2} = 0.83$ % (*1*) and 0.31 % (*2*). $R(bi - Xi)$, $P(bi - Xi)$ are the profiles of the O_2 (b, $v = i$) $\rightarrow O_2$ (X, $v' = i$) $+ hv_j$ molecular oxygen emission bands, where i is the vibrational-level number and $j = 8, 9, 10$ is the transition number.

The values of the Franck–Condon coefficients q_{ij} for an O_2 molecule for $i \neq j$ are much smaller than for $i = j$. This complicates the detection of bands with $i \neq j$. In addition, for $i > j$ the $O_2(b, v = i) \rightarrow O_2(X, v' = j)$ emission bands fall within the region of intense I_2 luminescence on the $I_2(B) \rightarrow I_2(X)$ transition. The $O_2(b)$ emission bands at $j > i$ shift to longer wavelengths, and their detection is impeded because of the low sensitivity of photodetectors in this wavelength range.

The emission band centred at 762 nm belongs to transition (8). Its intensity far exceeds the intensities of the transitions centred at 771 and 780 nm corresponding to processes (9) and (10), respectively. The emission intensity in the P branch for transition (10) is comparable to the noise of the detecting instruments. An additional emission band centred at $\lambda \approx 774$ nm overlaps the $P(b1 - X1)$ transition profile. The intensity of this band increases with the initial fraction η_{I_2} of molecular iodine. The emission bands for transitions (8)–(10) in the R branches are clearly observed and are not overlapped by other emission bands.

The radiation intensity I_{bi-Xi} of the $bi - Xi$th band is proportional to the product $\sigma_m^3 q_{i,i} N_{bi}$ [1], where σ_m is the wave number of the mth transition and N_{bi} is the concentration of $O_2(b, v = i)$ oxygen. Let us find the ratio of the concentrations of vibrationally excited molecules at the first and second vibrational levels to the concentration at the ground level:

$$\eta_{b1} = \frac{N_{b1}}{N_{b0}} = \frac{\sigma_8^3 I_{R(b1-X1)} q_{0,0}}{\sigma_9^3 I_{R(b0-X0)} q_{1,1}}, \quad \eta_{b2} = \frac{N_{b2}}{N_{b0}} = \frac{\sigma_8^3 I_{R(b2-X2)} q_{0,0}}{\sigma_{10}^3 I_{R(b0-X0)} q_{2,2}},$$

where $I_{R(bi-Xi)}$ is the signal intensity of the R branch for $v = i$. The values $\sigma_8^3 q_{0,0} = 2.103 \times 10^{12}$, $\sigma_9^3 q_{1,1} = 1.729 \times 10^{12}$ and $\sigma_{10}^3 q_{2,2} = 1.373 \times 10^{12}$ are taken from Ref. [18].

Fig. 3a shows the experimental dependence of the relative population η_{b1} of $O_2(b)$ at the first vibrational level on the initial relative content η_{I_2} of molecular iodine at a distance of 5 cm from the end of the nozzle assembly along the flow at gas pressures in the singlet-oxygen generator $p_g \approx 35$ Torr and in the measurement cell $p_c \approx 3$ Torr, respectively. The maximum fraction of vibrationally excited oxygen $\eta_{b1} \approx 22$ % is achieved at an iodine content of ~ 1 % in the oxygen flow. A further increase in η_{I_2} leads to a slight decrease in η_{b1}. Fig. 3b shows a similar plot for the relative population η_{b2} of $O_2(b)$ at the second vibrational level under the same conditions. Its behaviour is similar to that of η_{b1}. Thus, the maximum fraction of the vibrationally excited $O_2(b)$ molecules was 22 % and 10 % for the first and second vibrational levels, respectively.

Fig. 4 shows the measured relative content η_{b1} of $O_2(b)$ at the first vibrational level as a function of the coordinate L along the flow. The η_{b1}values weakly increase with L increasing from 2 to 5 cm and remain almost constant for $L = 5 - 9$ cm. Immediately behind the nozzle assembly at $L < 2$ cm in the measurement cell, an intense glow of molecular iodine was observed. Its emission intensity in the vicinity of 760 nm is of the same order of magnitude as that of oxygen on transitions (9) and (10); therefore, we failed to measure η_{b1} for $L < 2$ cm.

Reaction (2) has a much higher rate than reaction (1). Therefore, the $O_2(b)$ vibrational levels are predominantly populated in reaction (2). The difference of electron-

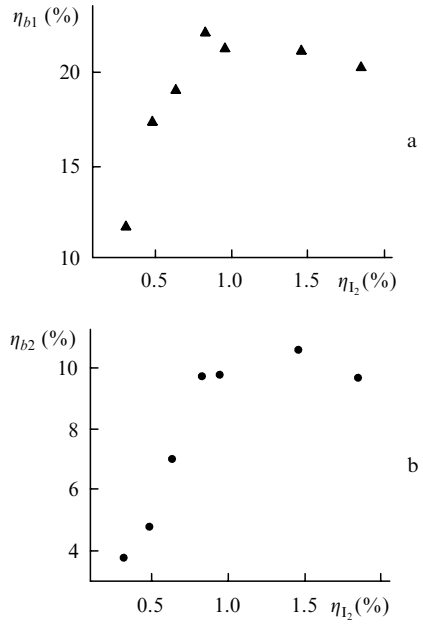

Figure 3. Relative population of electronically excited $O_2(b)$ oxygen at the (a) first η_{b1} and (b) second η_{b2} vibrational levels as a function of the relative initial concentration I_2 in oxygen at $p_g \approx 35$ Torr, $p_c = 3$ Torr, and $L = 5$ cm.

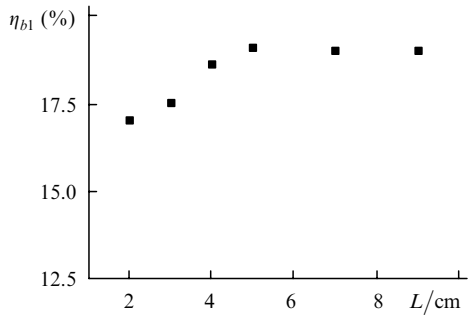

Figure 4. Relative population at the η_{b1} first vibrational level of $O_2(b)$ as a function of the coordinate L along the flow at $p_g \approx 30$ Torr, and $p_c = 3$ Torr.

excitation energies between the initial and final products of process (2) is 2364 cm^{-1}. The released-energy distribution over the reaction products is unknown. Assume that the probabilities of $O_2(b)$ formation with $v = 0$, 1 and 2 are γ_{b0}, γ_{b1} and γ_{b2}, respectively. The most effective redistribution of vibrational energy quanta between oxygen molecules $O_2(a)$, $O_2(b)$, and $O_2(X)$ occurs during the following EE energy-exchange processes:

$$O_2(b, v = 1) + O_2(a, v' = 0) \leftrightarrow O_2(a, v = 1) + O_2(b, v' = 0) - 79\ cm^{-1}, \quad (11)$$

$$O_2(b, v = 1) + O_2(X, v' = 0) \leftrightarrow O_2(X, v = 1) + O_2(b, v' = 0) - 151\ cm^{-1}, \quad (12)$$

$$O_2(b, v = 2) + O_2(a, v' = 0) \leftrightarrow O_2(a, v = 2) + O_2(b, v' = 0) - 159\ cm^{-1}, \quad (13)$$

$$O_2(b, v = 2) + O_2(X, v' = 0) \leftrightarrow O_2(X, v = 2) + O_2(b, v' = 0) - 307\ cm^{-1}, \quad (14)$$

$$O_2(a, v = 1) + O_2(X, v' = 0) \leftrightarrow O_2(X, v = 1) + O_2(a, v' = 0) - 72\ cm^{-1}, \quad (15)$$

$$O_2(a, v = 2) + O_2(X, v' = 0) \leftrightarrow O_2(X, v = 2) + O_2(a, v' = 0) - 148\ cm^{-1}. \quad (16)$$

The rate constants for the EE exchange between $O_2(b, v = 1, 2)$ and $O_2(X)$ molecules [processes (12) and (14)] were measured in Refs [19, 20]. Table 1 shows that $K_{12} > K_{14}$. According to Refs [19, 20], this is associated with the higher value of the energy defect in process (14).

Table 1.

Rate constant K_i ($cm^3\ s^{-1}$)	References
$K_1 = 2 \times 10^{-17}$	[21]
$K_2 = 1.1 \times 10^{-13}$	[22]
$K_3 = 6.7 \times 10^{-12}$	[23]
$K_4 = 2.3 \times 10^{-12}$	[24]
$K_5 = 3 \times 10^{-11}$	[25]
$K_{12} = 1.52 \times 10^{-11}$	[19]
$K_{14} = 2.7 \times 10^{-12}$	[20]
$K_{15} = 1.7 \times 10^{-11}$	[26]
$K_{17} = 10^{-13}$	[27, 28]
$K_{18}^{O_2} \approx 10^{-18}$	[29]
$K_{18}^{H_2O} \approx 10^{-16}$	[30]
$K_{19} = 3 \times 10^{-13}$	[15]
$K_{20} = 5 \times 10^{-11}$	[31]

The rate constants for the VV-exchange reactions

$$O_2(v) + O_2(v') \leftrightarrow O_2(v - 1) + O_2(v' + 1), \quad (17)$$

were measured for the first time in Ref. [27] and turned out to be several orders of magnitude lower than those for the EE-exchange processes (12) and (14). A distinguishing feature of the oxygen medium is the low VT-relaxation rate on the M components of the COIL active medium (O_2, N_2, and H_2O):

$$O_2(v) + M \leftrightarrow O_2(v - 1) + M. \quad (18)$$

The reserve of oxygen vibrational energy decreases through losses of vibrational energy quanta during the VV′ exchange with H_2O molecules:

$$O_2(v) + H_2O(000) \leftrightarrow O_2(v - 1) + H_2O(010). \quad (19)$$

Vibrationally excited water molecules are deactivated during the fast VT process:

$$H_2O(010) + H_2O \leftrightarrow H_2O(000) + H_2O. \quad (20)$$

High concentrations of vibrationally excited oxygen $O_2(b, v = 1, 2)$ were revealed in the experiment. These states are populated through two channels: by the excitation in the pooling reaction (2) and through an energy-quanta exchange in the EE processes (11)–(14). The contribution of the second channel increases with an increase in the average amount of vibrational quanta in O_2 molecules. Steady-state concentrations N_{b0}, N_{b1} and N_{b2} can be determined from balance equations for the formation and deactivation of vibrationally excited oxygen at levels $v = 0, 1, 2$:

$$\gamma_{b0}K_2N_aN_{I^*} + K_{11}^+N_{a0}N_{b1} + K_{12}^+N_{X0}N_{b1} + K_{13}^+N_{a0}N_{b2} + K_{14}^+N_{X0}N_{b2} = K_3N_{b0}N_w + K_{11}^-N_{b0}N_{a1} + K_{12}^-N_{b0}N_{X1} + K_{13}^-N_{b0}N_{a2} + K_{14}^-N_{b0}N_{X2}, \quad (21)$$

$$\gamma_{b1}K_2N_aN_{I^*} + K_{11}^-N_{b0}N_{a1} + K_{12}^-N_{b0}N_{X1} = K_{11}^+N_{a0}N_{b1} + K_{12}^+N_{X0}N_{b1}, \quad (22)$$

$$\gamma_{b2}K_2N_aN_{I^*} + K_{13}^-N_{b0}N_{a2} + K_{14}^-N_{b0}N_{X2} = K_{13}^+N_{a0}N_{b2} + K_{14}^+N_{X0}N_{b2}, \quad (23)$$

where K_i^+ and K_i^- are the rate constants for the forward and reverse ith reactions; N_{ai} and N_{Xi} are the concentrations of $O_2(a, v = i)$ and $O_2(X, v = i)$; and N_w, N_{I^*} are the concentrations of H_2O and I^*. The rates of processes (17) and (18) are much lower than the rates of processes (11)–(16); therefore, they are not included in balance equations (21)–(23). Expressing N_{b1} from (22) and N_{b2} from (23) and substituting them into (21), we obtain

$$N_{b0} = \frac{K_2N_aN_{I^*}}{K_3N_w}. \quad (24)$$

Thus, the steady-state concentration of $O_2(b, v = 0)$ is determined by the $O_2(b)$ production rate in pooling reaction (2) and its deactivation rate in process (3). Using the steady-state condition for fast processes (15) and (16), we can obtain the relations

$$N_{X1} = \frac{K_{15}^+N_{X0}}{K_{15}^-N_{a0}}N_{a1}, \quad N_{X2} = \frac{K_{16}^+N_{X0}}{K_{16}^-N_{a0}}N_{a2}. \quad (25)$$

Let us pass from the absolute concentrations to relative populations: $\eta_w = N_w/N_{O_2}$, $\eta_{a0} = N_{a0}/N_{O_2}$, $\eta_{X0} = N_{X0}/N_{O_2}$, $\eta_{a1} = N_{a1}/N_{a0}$, and $\eta_{a2} = N_{a2}/N_{a0}$. To simplify the consideration, we introduce the notation $Q = N_{X0}/N_{a0}$, $\beta_1 = K_{12}^-/K_{11}^- \approx K_{12}^+/K_{11}^+$, $\beta_2 = K_{14}^-/K_{13}^- = K_{14}^+/K_{13}^+$ and take into account that $K_{11}^+/K_{11}^- = \exp(-114/T)$, $K_{13}^+/K_{13}^- = \exp(-229/T)$, $K_{15}^+/K_{15}^- = \exp(-104/T)$, and $K_{16}^+/K_{16}^- = \exp(-213/T)$. Using relations (21)–(25), we obtain the following equations for the fractions of vibrationally excited $O_2(b)$ with $v = 1$ and 2:

$$\eta_{b1} = \frac{N_{b1}}{N_{b0}} = \frac{\gamma_{b1}K_3\eta_w}{K_{11}^+\eta_{a0}(1 + \beta_1Q)} + \exp(114/T) \times \left[\frac{1 + \beta_1Q\exp(-104/T)}{1 + \beta_1Q}\right]\eta_{a1}, \quad (26)$$

$$\eta_{b2} = \frac{N_{b2}}{N_{b0}} = \frac{\gamma_{b2}K_3\eta_w}{K_{13}^+\eta_{a0}(1 + \beta_2Q)} + \exp(229/T) \times \left[\frac{1 + \beta_2Q\exp(-213/T)}{1 + \beta_2Q}\right]\eta_{a2}. \quad (27)$$

The first terms in Eqns 26) and (27) define the fractions of vibrationally excited $O_2(b)$ determined by the excitation in pooling reaction (2). The second terms define the fractions of $O_2(b, v = 1, 2)$ determined by the redistribution of vibrational energy quanta between $O_2(a)$, $O_2(b)$, and $O_2(X)$ molecules during fast EE-exchange processes (11)–(16). The rate constants for the EE exchange between $O_2(b)$ and $O_2(a)$ molecules in processes (11) and (13) are unknown. The energy defect in process (11) is smaller than in similar process (12). The same is valid for processes (13) and (14). A tendency to an increase in the rate with a decrease in the energy defect of the EE-exchange reaction was noted in Refs [19, 20] and indicates that $K_{12}/K_{11} < 1$ and $K_{14}/K_{13} < 1$. The energy defect in processes (12) and (13) is virtually the same (~ 151 and $159\ cm^{-1}$). It can be assumed that $K_{13}^+ \approx K_{12}^+$.

Let us analyse Eqns (26) and (27). Under conditions of the performed experiments, $\eta_{b1} \approx 0.22$, $\eta_{b2} \approx 0.1$, $\eta_w \approx 0.04$, $\eta_{a0} \approx 0.5$, $Q \approx 1$, and $T \approx 400$ K. Under such conditions, the contribution of the first terms does not exceed 0.01 even at $\gamma_{b1} = \gamma_{b2} = 1$. The values of the expressions in brackets of the second terms of (26) and (27) are close to unity. As a result, the following approximate formulas can be written:

$$\eta_{b1} \approx \eta_{a1}\exp(114/T), \ \eta_{b2} \approx \eta_{a2}\exp(229/T).$$

From here, the fractions of vibrationally excited singlet oxygen are $\eta_{a1} \approx 17\,\%$ and $\eta_{a2} \approx 6\,\%$. The average amount of vibrational quanta in the oxygen–iodine medium under study is $\eta_v = \sum_n n\eta_n \approx 30\,\%-40\,\%$ (η_n is the fraction of vibrationally excited O_2 at the nth vibrational level, $n = 1, 2, 3, \ldots$.

4. Conclusions

The emission technique makes it possible to detect vibrationally excited O_2 and determine its quantitative content in the COIL active medium. The emission bands of electronic–vibrational–rotational transitions of O_2 molecules (8)–(10) fall within the visible wavelength region, in which the I_2 emission intensity on the $I_2(B) \rightarrow I_2(X)$ transition is minimum. In the reaction zone behind the nozzle assembly at a distance of a few centimetres downstream, where the concentration of I_2 is still high, the emission intensity on this transition is of the same order of magnitude as that of bands (9) and (10). This circumstance did not allow measurements in the I_2 dissociation region to be performed.

In our experiments, the relative content of vibrationally excited $O_2(b)$ molecules in an $O_2(a)$–I medium, whose composition is close to that of the COIL active medium, was $\eta_{b1} \approx 22\,\%$ and $\eta_{b2} \approx 10\,\%$ for the first and second vibrational levels, respectively. The maximum content of $O_2(b, v)$ was observed at a relative initial fraction of I_2 in O_2 of $\sim 1\,\%$. The relative concentration of vibrationally excited oxygen slightly decreases with the distance along the flow direction.

Vibrational levels of O_2 are excited in processes (2) and (3). Due to the fast EE energy exchange in processes (11)–(16), the degrees of vibrational excitation of $O_2(X\,^3\Sigma_g^-)$,

$O_2(a\,^1\Delta_g)$ and $O_2(b\,^1\Sigma_g^+)$ oxygen molecules are almost identical. Using the experimentally measured relative populations η_{b1} and η_{b2} for $O_2(b)$ from (26) and (27), we can find the relative populations for singlet oxygen at $v = 1$ and 2. For the $N_2 : O_2 : I_2 : H_2O = 100 : 100 : 1 : 4$ active medium composition, a partial oxygen pressure of 1.5 Torr, and $T \approx 400$ K, the maximum relative singlet-oxygen populations for the first and second levels were $\sim 17\,\%$ and $\sim 6\,\%$, respectively.

The rates of the VT relaxation of vibrationally excited O_2 on the medium components are rather low. The $O_2(v)$ deactivation rate is limited by the VV exchange with the H_2O bending mode [process (19)]. The content of vibrationally excited O_2 will presumably increase with a decrease in the fraction of water vapours.

In EV process (4), vibrationally excited $H_2O(002)$ water molecules are produced. The $H_2O(010)$ state is predominantly populated during the fast VV exchange between the valence and bending modes. Oxygen and water molecules exchange with vibrational energy quanta during process (19). It can be asserted that the population of vibrationally excited H_2O states in the COIL active medium is also nonequilibrium.

Hence, using the emission technique, we have shown for the first time that a mean number of vibrational quanta per one O_2 molecule in the COIL active medium reaches 30 %. This fact is an additional argument in favour of the I_2 dissociation model in which vibrationally excited oxygen participates in populating intermediate excited iodine electronic states $I_2(A')$ and $I_2(A)$ [processes (6) and (7)].

Since the fraction of vibrationally excited $O_2(a,\ v)$ molecules is rather large, apart from $O_2(a,\ v = 0)$ participating in the process

$$O_2(a, v = 0) + I \leftrightarrow O_2(X, v = 0) + I^* + 279\ \mathrm{cm}^{-1} \qquad (28)$$

vibrationally excited $O_2(a,\ v = 1)$ and $O_2(a,\ v = 2)$ singlet-oxygen molecules participate in the inversion of the laser transition in the COIL in the processes

$$O_2(a, v = 1) + I \leftrightarrow O_2(X, v = 1) + I^* + 207\ \mathrm{cm}^{-1}, \qquad (29)$$

$$O_2(a, v = 2) + I \leftrightarrow O_2(X, v = 2) + I^* + 131\ \mathrm{cm}^{-1}. \qquad (30)$$

The rate constants for reactions (29) and (30) are unknown. The energy-defect and equilibrium-constant values in processes (28)–(30) decrease with an increase in the vibrational-level number. The spin–orbital transition of an iodine atom is inverted in each of processes (28)–(30), if the corresponding threshold of singlet oxygen yield are equal to 15, 20, and 26 % for (28), (29), and (30). The total threshold of $O_2(a)$ yield must be higher than the conventional value.

The theoretical COIL models must involve processes with the participation of vibrationally excited O_2 molecules. Reactions (6) and (7) may play an important role in the I_2 dissociation process. When calculating the gain and the threshold of singlet oxygen yield, along with (28), processes (29) and (30) should be taken into consideration. Unfortunately, the released-energy distribution between the reaction products in processes (2) and (3) and rate constants for processes (6), (7), (11), (13), (29) and (30) are unknown. This will complicate the theoretical simulation of kinetic processes in oxygen–iodine lasers.

References

1. Schurath U. *J. Photochem.*, **4**, 215 (1975).
2. Thomas R.G.O., Thrush B.A. *Proc. R. Soc. Lond. A.*, **356**, 295 (1977).
3. Thomas R.G.O., Thrush B.A. *Proc. R. Soc. Lond. A.*, **356**, 307 (1977).
4. Grimley A.J., Houston P.L. *J. Chem. Phys.*, **69**, 2339 (1978).
5. Van Betchem M.H., Davis S.J. *J. Phys. Chem.*, **90**, 902 (1986).
6. Hall G.E., Marinelli W.J., Houston P.L. *J. Phys. Chem.*, **87**, 2153 (1983).
7. Azyazov V.N., Igoshin V.I., Kupriyanov N.L. *Krat. Soobshch. Fiz.*, (1–2), 24 (1992).
8. Azyazov V.N., Pichugin S.Yu., Safonov V.S., Ufimtsev N.I. *Kvantovaya Elektron.*, **31**, 794 (2001) [*Quantum Electron.*, **31**, 794 (2001)].
9. David D. *Chem. Phys. Lett.*, **93**, 16 (1982).
10. Heidner III R.F., Gardner C.E., Segal G.I., El-Sayed T.M. *J. Phys. Chem.*, **87**, 2348 (1983).
11. Bohling R., Becker A.C., Minaev B.F., Seranski K., Schurath U. *Chem. Phys.*, **142**, 445 (1990).
12. Komissarov A.V., Goncharov V., Heaven M.C. *Proc. SPIE Int. Soc. Opt. Eng.*, **4184**, 7 (2001).
13. Derwent R.G., Thrush B.A. *Trans. Farad. Soc.*, **68**, 720 (1972).
14. Biryukov A.S., Shcheglov V.A. *Kvantovaya Elektron.*, **13**, 510 (1986) [*Sov. J. Quantum Electron.*, **16**, 333 (1986)].
15. Azyazov V.N., Nikolaev V.D., Svistun M.I., Ufimtsev N.I. *Kvantovaya Elektron.*, **28**, 212 (1999) [*Quantum Electron.*, **29**, 767 (1999)].
16. Azyazov V.N., Safonov V.S., Ufimtsev N.I. *Kvantovaya Elektron.*, **30**, 687 (2000) [*Quantum Electron.*, **30**, 687 (2000)].
17. Azyazov V.N., Safonov V.S., Ufimtsev N.I. *Kvantovaya Elektron.*, **32**, 799 (2002) [*Quantum Electron.*, **32**, 799 (2002)].
18. Krupenie P.H. *J. Phys. Chem. Ref. Data*, **1**, 423 (1972).
19. Bloemink H.I., Copeland R.A., Slanger T.G. *J. Chem. Phys.*, **109**, 4237 (1998).
20. Kalogerakis K.S., Copeland R.A., Slanger T.G. *J. Chem. Phys.*, **116**, 4877 (2002).
21. Derwent R.G., Thrush B.A. *Trans. Farad. Soc.*, **67**, 2036 (1971).
22. Heidner III R.F., Gardner C.E., El-Sayed T.M., Segal G.I., Kasper J.V.V. *J. Chem. Phys.*, **74**, 5618 (1981).
23. Aviles R.G., Muller D.F., Houston P.L. *Appl. Phys. Lett.*, **37**, 358 (1980).
24. Burde D.H., McFarlane R.A. *J. Chem. Phys.*, **64**, 1850 (1976).
25. Cline J.I., Leone S.R. *J. Phys. Chem.*, **95**, 2917 (1991).
26. Jones I.T.N., Bayes K.D. *J. Chem. Phys.*, **57**, 1003 (1972).
27. Kalogerakis K.S., Copeland R.A., Slanger T.G. *Eos. Trans. AGU*, **82** (47), SA41B-0728 (2001).
28. Coletti C., Billing G.D. *Chem. Phys. Lett.*, **356**, 14 (2002).
29. Parker J.G., Ritke D.N. *J. Chem. Phys.*, **59**, 3713 (1973).
30. Britan A.B., Starik A.M. *J. Prikl. Met. Teor. Fiz.*, **4**, 41 (1980).
31. Finzi J., Hovis F.E. *J. Chem. Phys.*, **67**, 4053 (1977).